Check for updates

Extraction optimization and quality evaluation of humic acids from lignite using the cell-free filtrate of *Penicillium ortum* MJ51†

Shiying Li,‡[ab] Jinfang Tan,‡[c] Yi Wang,[b] Peipei Li,[b] Desheng Hu,[b] Qiuzhe Shi,[b] Yanjun Yue,[d] Fang Li*[b] and Yanlai Han ⓘD *[b]

Bio-solubilization of lignite is a promising technology to transform coal into humic acids (HAs) which are broadly used in agriculture. In this work, HAs were extracted from lignite using the cell-free filtrate (CFF) of *Penicillium ortum* MJ51. The extraction method was optimized using response surface methodology (RSM) based on the interactive effects of nitric acid concentrations, coal loading ratio, extraction temperature and time as input factors, and the absorbance of HAs at 450 nm wavelength as the output response. Under optimized conditions (lignite pretreated with 4.7 N HNO_3, coal loading ratio of 4.9%, temperature of 77.3 °C and time of 8.6 hours), the absorbance at 450 nm peaked at 70.28, and the concentration and extraction yield of HAs were 31.3 g L^{-1} and 63.9%, respectively, which were dramatically higher than those observed for traditional biological methods (0.7 g L^{-1} and 14.1%, respectively). The qualities of HAs produced under optimized conditions were evaluated and compared with those extracted by the conventional chemical method. The optimized process resulted in better HA quality indices, including lower molecular mass; higher nitrogen; less aromatic carbon; more aliphatic and carboxylic carbon; and higher bioactivity for promoting plant growth. Moreover, the anti-flocculation ability was improved, thereby supporting its applicability in agriculture. Extraction of HAs from lignite using the CFF of *P. ortum* MJ51 provides a novel technological approach for the efficient conversion of lignite to bio-active HAs.

1. Introduction

Humic acids (HAs) are a class of natural polyelectrolyte complexes with a large number of active groups, including carboxyl groups, phenolic hydroxyl groups, carbonyl groups and methoxy groups, the pressence of these groups endows HAs with many capabilities such as complexation, ion exchange and redox properties, and makes HAs widely used in various fields, especially agriculture.[1] As a fertilizer additive and soil remediation agent, HAs play an important role in stimulating plant growth, enhancing soil fertility and decreasing the toxicity of heavy metals.[2–4] Accordingly, the potential biochemical activity and preparation method of HAs have aroused extensive attention.

[a]Collaborative Center Innovation of Henan Food Crops, Henan Agricultural University, Zhengzhou 450002, China

[b]College of Resources and Environmental Science, Henan Agricultural University, Zhengzhou 450002, China. E-mail: fangli0901@henau.edu.cn; hyanlai@henau.edu.cn

[c]School of Agriculture, Sun Yat-sen University, Guangzhou 510000, China

[d]Henan Xinlianxin Chemicals Group Co., Ltd, Xinxiang 453000, China

† Electronic supplementary information (ESI) available. See DOI: 10.1039/d1ra08019a

‡ The first two authors contributed equally to this study.

Lignite, a kind of low rank coal is an energy source as well as a HAs resource, accounts for 45% of the global low-rank coal reserves.[5] Efforts had been made to extract HAs from lignite *via* chemical and biological methods.[6–8] The amount of HAs extracted chemically depends on the extraction agent (such as NaOH or KOH), temperature, time and coal particle size.[42] Although chemical methods are efficient, HAs prepared *via* biological methods are more environmentally safe and have better bioactivity.[9] Esterase-degraded lignite HAs have a higher percentage of aliphatic carbon, but a lower percentage of aromatic carbon and ester groups than raw lignite HAs, and have been shown to promote the growth of asparagus lettuce.[10] Oxidation pretreatment of lignite can also improve HA bioactivity by reducing their molecular weight and increasing their content of active functional groups.[11] Among a variety of oxidants (such as hydrogen peroxide, nitric acid and sodium hydroxide), nitric acid (HNO_3) was the most effective pretreatment to improve the oxidation degree of coal.[12] Oxidizing pretreatment of coal with HNO_3 also promotes microbial solubilization of coal, enhances the yield of HAs and the number of oxygen and nitrogen functional groups.[7,13] Combining an oxidation pretreatment of coal with biological methods to obtain HAs of high quantity and quality has become a promising research area.

In the 1980s, white-rot fungi were reported to dissolve coal.[14] Since then, many microorganisms, including *Bacillus* sp. Y7,[15] *Penicillium* sp. P6 [16] and *Streptomyces fulvissimus* K59,[18] have been reported to convert low-rank coal into HAs. Generally, microorganisms degrade coal by releasing extracellular metabolites, such as surfactants, alkaline substances and extracellular enzymes.[19] Due to the diversity of microorganisms that produce various extracellular metabolites, the mechanism and efficiency of coal bio-solubilization vary. A recent study revealed that 35% of H_2O_2-pretreated lignite was solubilized by *Trichoderma citrinoviride*, which can secret oxidase, lignin peroxidase and laccase.[20] Another study obtained a higher bio-solubilization rate (36.77%) using the thermostable, alkaline extracellular materials produced by *Bacillus* sp. Y7.[15] Furthermore, it has been shown that lignite components can be solubilized using biosurfactant-containing cell-free filtrate (CFF) extracted from *Bacillus licheniformis*.[21] Most coal-solubilizing bacteria and actinomycetes primarily rely on alkaline action and chelation, while fungi mostly rely on enzymes, but also utilize the above substances to a lesser degree.[22,23] Although extracellular metabolites are widely known for their role in the lignite solubilization process, research on process optimization of HA extraction from lignite using extracellular CFF is still scarce.

Nowadays, efforts had been made to improve the yield and bioactivity of HAs. The amount of HAs produced *via* biological methods is influenced by the culture conditions, temperature, time, coal particle size, coal loading ratio and oxidation content of coal.[17,24] Accordingly, an appropriate experimental design is necessary to optimize the extraction conditions. Response surface methodology (RSM) has been widely used to explore the optimal conditions related to multiple factors.[25,26] RSM modeling describes the relationship between input and response variables with advantage of minimizing the number of experimental runs.[27] Hence, RSM could be adopted to optimize the conditions for HA production. The biochemical activity of HAs is determined by their chemical composition, structure, molecular weight and other properties.[28,29] To investigate the chemical and structural properties of HAs, numerous analytical methods have been widely used, including elemental analysis, titration analysis of acidic functional groups, ultraviolet-visible (UV-Vis) spectroscopy, fluorescence spectra, Fourier transform infrared (FTIR) spectroscopy, cross polarization magic angle spinning ^{13}C NMR (CP/MAS ^{13}C NMR) spectrometry, X-ray diffraction (XRD), gas chromatography-mass spectrometry (GC-MS), high-performance size-exclusion chromatography (HPSEC) and scanning electron microscopy (SEM).[30–33]

Here, *Penicillium ortum* MJ51 was isolated from lignite, which has strong ability to solubilize lignite. Some strains of *Penicillium* spp., such as *P. simplicissimum*, *P. citrinum* and *P. decumbens* P6 are reportedly able to solubilize and degrade lignite.[22,34,35] However, the extraction of HAs from lignite using the CFF of the *P. ortum* strain has not been conducted yet. In view of the important role of extracellular metabolites secreted by microorganisms in lignite solubilization, it can be hypothesized that extracellular CFF of *P. ortum* MJ51 could be used to extract HAs from lignite and that HAs have better bioactivity than that extracted by traditional chemical methods. To test this hypothesis, HAs were extracted from lignite using the CFF of *P. ortum* MJ51, the extraction conditions were optimized through RSM based on the interactive effects of the input factors (specifically, HNO_3 concentration, coal loading ratio, extraction temperature and time) and the output response (specifically, the absorbance of HAs at 450 nm wavelength). Meanwhile, the quality of HAs extracted under optimized conditions was evaluated and compared with that extracted by conventional chemical methods *via* elemental analysis, flocculation, HPSEC, FTIR spectroscopy and CP/MAS ^{13}C NMR spectroscopy.

2. Materials and methods

2.1. Coal samples

The coal samples used in this experiment were collected from the Mile Coal Mine in Yunnan Province, China, and then transported to the laboratory and stored at 4 °C. The coal samples were ground to a diameter of 0.18–0.25 mm and dried to a constant weight in an oven at 80 °C. Chemical characterization of the coal samples, which included proximate analysis, calorific value and vitrinite reflectance, was performed according to Sabar *et al.* (2019).[17] The gross calorific value and vitrinite reflectance of the coal were measured using a 5E-C5508 Kaiyuan Calorimeter (Changsha, China) and a Leitz Orthoplan microscope (Solms, Germany), respectively. The ash and volatile contents of the coal samples were 29.5% and 44.04%, respectively, and the gross calorific value and vitrinite reflectance index were 18.63 MJ kg^{-1} and 0.39%, respectively. These results indicate that the coal was meta-lignite.

2.2. Fungus and cell-free filtrate (CFF)

Penicillium ortum MJ51, which was isolated from fresh lignite samples, has 99% sequence homology of the internal transcribed spacer (ITS) region with the *P. ortum* strain MK450708.1. This strain has been demonstrated to effectively degrade coal (unpublished data).

The fungal strain MJ51 was inoculated on potato dextrose agar (PDA; 200 g potato, 20 g glucose, 20 g agar and 1000 mL distilled water) and cultivated for 6 d at 28 °C. After cultivation, 0.1% sterilized NaCl was added to form a spore suspension. The number of spores was observed under a microscope using a hemocytometer. Next, 2.5 mL of spore suspension (1×10^8 spores per mL) was inoculated into a 250 mL flask containing 50 mL of culture fluid (20.0 g L^{-1} sucrose, 3 g L^{-1} KNO_3, 1 g L^{-1} KH_2PO_4, 0.5 g L^{-1} Na_2HPO_4, 0.5 g L^{-1} $MgSO_4\cdot7H_2O$; pH 6.0). The inoculated medium was cultured at 160 rpm and 30 °C. The CFF obtained from the different fermentation times (12 hours intervals) was prepared by centrifuging 50 mL of the culture at 12 000g for 10 min. The pH of the CFF was measured and the mycelium was dried to a constant weight at 75 °C.

2.3. Optimization of the HA production process

The CFF (20 mL) was incubated with lignite in a 50 mL flask in a SHA-CA reciprocating water bath oscillator (Changzhou, China). Different parametric effects for HA production were

Table 1 Different conditions for bio-solubilization experiment

Group	Variables	Ranges	Conditions
1	Bio-solution type	A: culture solution inoculation with *P. ortum* MJ51 for 0 hour B: CFF of *P. ortum* MJ51 cultured to the 60th hour	0.5% raw lignite, 30 °C, 160 rpm
2	Incubation time	0 h, 12 h, 24 h, 36 h, 48 h, 60 h, 72 h, 84 h, 96 h, 108 h, 120 h, 132 h, 144 h, 156 h, 168 h	0.5% raw lignite, 30 °C, 160 rpm
3	Temperature	30 °C, 45 °C, 60 °C, 75 °C, 90 °C	0.5% raw lignite, 160 rpm
4	HNO$_3$ concentration	0 N, 0.5 N, 1 N, 2 N, 4 N, 6 N	0.5% raw lignite, 75 °C, 160 rpm
5	Coal loading ratio	0.5%, 1%, 2%, 3%, 4%, 5%, 6%	4 N HNO$_3$, 75 °C, 160 rpm

studied, including the bio-solution type, fungal growth phase, HNO$_3$ concentration for coal pretreatment, coal loading ratio, temperature and time; see Table 1 for the specific conditions. Pretreated lignite samples were prepared by placing raw lignite into HNO$_3$ at a ratio of 1 g coal per 25 mL solution. Pretreatments were performed using 0, 0.5, 1, 2, 4, 6 N HNO$_3$. Chemical pretreatment was conducted in 50 mL glass vials at 30 °C for 48 hours. After pretreatment, the samples were centrifuged at 7000*g* for 10 min and then washed with deionized water until the filtrate was colorless and the pH was greater than 5. Finally, the treated coal was dried in an oven at 80 °C.

For the solubilization study, three groups of parallel experiments were performed. After solubilization, the samples were centrifuged at 8000*g* for 12 min, and the content of coal solubilization products in the supernatant was determined using a Thermo Scientific UV1510 Spectrophotometer (Waltham, USA) at a wavelength of 450 nm, which is related to the HA content.[18]

The optimal condition for HA extraction from lignite was determined by the Box–Behnken design of RSM. Based on the univariate analysis, ranges for variable value design of the RSM were as follows: HNO$_3$ concentration: 2, 4, 6 N; coal loading ratio: 4, 5, 6%; time: 6, 8, 10 h; and temperature: 60, 75, 90 °C. Variables and experimental design of the RSM are shown in Tables 2 and 3. The RSM design was analyzed by Design-Expert 8.0 software.

2.4. Concentration and extraction yield of HAs

HAs were extracted from raw lignite, HNO$_3$-pretreated lignite with 60 h CFF (HA-CFF), and 0.1 M NaOH solution as the control (HA-control). The volume of extractant was 20 mL. The method for HA extraction was modified from Sabar *et al.* (2020).[9] The specific HNO$_3$ concentration used for pretreating lignite, coal loading ratio, extraction time and temperature referred to the optimum conditions of RSM. The HA concentration and yield

were determined gravimetrically as per eqn (1) and (2), respectively.

$$C_{HAs}\ (g\ L^{-1}) = \frac{wt.\ of\ dried\ HAs}{v.\ of\ extractant} \times 100 \quad (1)$$

$$HA\% = \frac{wt.\ of\ dried\ HAs}{wt.\ of\ dried\ coal} \times 100 \quad (2)$$

2.5. Quality evaluation of HAs

2.5.1. Elemental analysis, E_4/E_6 ratio analysis and molecular weight distribution of HAs. Elemental composition of the extracted HAs was determined with an Elementar Vario EL cube (Hanau, Germany). The oxygen content was calculated by determining the difference. The E_4/E_6 ratio was determined by taking the ratio of absorbances at 465 and 665 nm. The molecular weight distribution of HAs was determined by HPSEC. The specific method was performed according to Sabar *et al.*, (2020).[9]

2.5.2. Flocculation limit. The flocculation limit represents the minimum milliequivalent number of electrolytes (0.1 mol L^{-1} CaCl$_2$) that must be added to the 0.02% HA lye solution in 1 hour. The specific protocol was as follows: HA samples were dissolved in a 0.05 M NaHCO$_3$ solution at pH 8.4 with a concentration of 20 mg HAs per 100 mL solution. A series of 0.1 mol L^{-1} CaCl$_2$ solutions of different volumes (0.2–1.0 mL, in 0.02 mL increments) was prepared; the CaCl$_2$ solution was then diluted to 2.5 mL with deionized water; 5 mL of the 0.02% HA solution was added into the CaCl$_2$ solutions of different concentrations; and then the solutions were left to stand for 1 hour. Finally, flocculation in the test tubes was observed. The calculation for the flocculation limit is described as eqn (3)

$$Flocculation\ limit\ (mmol\ L^{-1}) = M \cdot V \times 1000/5 = 200MV \quad (3)$$

where M is the CaCl$_2$ concentration (here 0.1 mol L^{-1}) and V is the minimum CaCl$_2$ addition amount (mL) at which the aggregation limit is reached.

2.5.3. Spectroscopy analysis of HAs. To investigate the structure and functional group distribution of the HA samples, FTIR and solid-state CP/MAS ^{13}C NMR analyses were performed. For FTIR, 2 mg HAs was thoroughly mixed with 200 mg dried KBr and pressed into pellets. The pellets were subjected to

Table 2 Range of values for response surface variables

Factor	Name	Units	Minimum	Maximum	Mean
A	HNO$_3$ concentration	N	2	6	4
B	Temperature	°C	60	90	75
C	Coal loading ratio	%	4	6	5
D	Time	hours	6	10	8

Table 3 Box–Behnken design with four-factor and three-level[a]

	Factor 1 A: HNO$_3$ concentration (N)		Factor 2 B: temperature (^{o}C)		Factor 3 C: coal loading ratio (%)		Factor 4 D: time (h)		
Run	Coded	Actual	Coded	Actual	Coded	Actual	Coded	Actual	A_{450}
1	0	4	−1	60	0	5	−1	6	50.36 ± 0.56
2	−1	2	0	75	1	6	0	8	26.34 ± 0.39
3	−1	2	−1	60	0	5	0	8	29.79 ± 0.40
4	0	4	0	75	0	5	0	8	68.61 ± 0.63
5	0	4	1	90	−1	4	0	8	59.87 ± 1.31
6	0	4	0	75	−1	4	−1	6	52.16 ± 0.84
7	0	4	−1	60	0	5	1	10	55.65 ± 1.09
8	−1	2	1	90	0	5	0	8	31.71 ± 0.32
9	1	6	0	75	−1	4	0	8	54.90 ± 1.51
10	−1	2	0	75	0	5	1	10	29.96 ± 0.72
11	0	4	0	75	1	6	−1	6	49.77 ± 0.34
12	0	4	0	75	−1	4	1	10	61.73 ± 1.18
13	0	4	0	75	0	5	0	8	68.02 ± 1.31
14	0	4	0	75	0	5	0	8	67.49 ± 1.24
15	0	4	0	75	0	5	0	8	65.45 ± 1.67
16	1	6	0	75	0	5	1	10	57.11 ± 0.74
17	0	4	1	90	1	6	0	8	51.95 ± 0.70
18	1	6	0	75	1	6	0	8	50.92 ± 1.49
19	−1	2	0	75	−1	4	0	8	26.89 ± 0.68
20	0	4	−1	60	1	6	0	8	45.96 ± 1.20
21	0	4	1	90	0	5	−1	6	56.40 ± 1.38
22	0	4	0	75	1	6	1	10	54.94 ± 0.94
23	1	6	−1	60	0	5	0	8	45.02 ± 0.71
24	0	4	−1	60	−1	4	0	8	51.26 ± 1.20
25	1	6	0	75	0	5	−1	6	52.20 ± 1.08
26	−1	2	0	75	0	5	−1	6	28.60 ± 0.48
27	1	6	1	90	0	5	0	8	55.92 ± 1.25
28	0	4	0	75	0	5	0	8	66.49 ± 1.49
29	0	4	1	90	0	5	1	10	64.68 ± 1.31

[a] Note: results are presented as the mean ± standard deviation.

FTIR scanning using a Nicolet IS10 FTIR spectrometer (Madison, USA) in the region of 4000–400 cm^{-1}. The solid-state CP/MAS ^{13}C NMR spectra of the HA samples were obtained using a Bruker AVANCE III 500 MHz spectrometer (Karlsruhe, German) at a resonance frequency of 100.63 MHz, magic angle spinning at 12 kHz, a contact time of 3.5 ms and pulse delay of 2 s. Approximately 1200 scans were performed for each spectrum. The spectral data of the HAs were quantitatively analyzed according to the literature.[36]

2.5.4. Effect of HAs on maize growth. To verify the effect of the HA biological activity on maize growth, two treatments with three replicates each were established, namely the HA-control and HA-CFF. Pots (20 cm × 25 cm) containing 7.5 kg of air-dried soil were arranged randomly. All treatments received the same amount of N, P$_2$O$_5$, K$_2$O and HAs (0.15, 0.1, 0.1 and 0.03 g kg^{-1}, respectively). Three maize seeds were sown in each pot. After 30 days, the stem diameter, plant height and biomass of the plants were measured.

3. Results and discussion

3.1. Optimization of HA extraction conditions

To enhance the release of water-soluble HAs from coal, crucial parameters that could potentially affect the concentration of dissolved coal products *via* coal solubilization were studied, including the fungal incubation time, HNO$_3$ concentration for coal pretreatment, coal loading ratio, reaction temperature and time.[17,18] The HA content was evaluated by measuring the absorbance value of bio-solubilized products at a wavelength of 450 nm (A_{450}), which is the characteristic UV/Vis absorbance wavelength of HAs.

3.1.1. Effect of fungal incubation time on untreated coal dissolution. Lignite bio-solubilization can occur in fermentation broths with both living microbial cells and without living cells. The latter mainly depends on the action of secondary metabolites,[37] which is more conducive to the optimized separation and extraction conditions of HAs. In this study, two types of biological solutions (A and B) were used to dissolve lignite. Solution A represents a culture solution inoculated with *P. ortum* MJ51 for 0 hours, and solution B represents the CFF of *P. ortum* MJ51 prepared after cultivation for 60 hours (the time at which the mycelial biomass peaked) (Fig. 1a). The A_{450} of the supernatant was measured from the moment when lignite was added to solutions A and B. The results (Fig. 1b) show that the A_{450} of the solution B supernatant increased sharply and peaked at the 4th hour, while that of the solution A supernatant only increased significantly at the 48th hour and then peaked on the 10th day. Furthermore, there was no significant difference
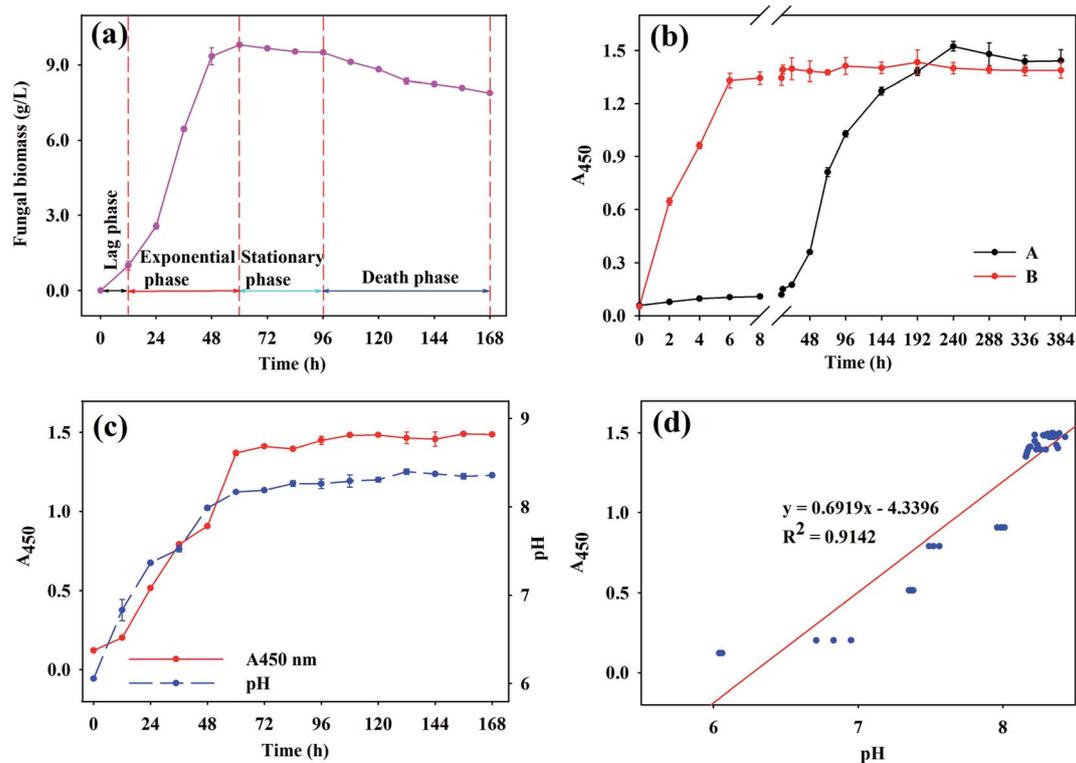
Fig. 1   (a) Growth curve of *Penicillium ortum MJ51* strain; (b) effect of bio-solution type (A: culture solution inoculation with *P. ortum* MJ51 for 0 hour; B: CFF of *P. ortum* MJ51 cultured to the 60th hour) on coal solubilization; (c) pH of the cell-free filtrate (CFF) with different culture time and lignite degradation in the CFF by *P. ortum MJ51*; (d) the relationship between pH of the CFF and the absorbance of HAs at 450 nm wavelength. Note: error bars indicate standard deviation.

between the maximum A_{450} of solutions A and B ($p < 0.05$). This phenomenon demonstrates that the CFF can promote the release of HAs more quickly. Other studies indicate that the optimal fungal incubation time to obtain the maximum release of organics from coal often exceeds 7 days,[17,38] which is consistent with the results seen for coal dissolution by solution A in this study. Efficient solubilization occurs in medium containing rich secondary metabolites, which largely accumulate when fungi grow to a certain extent. Accordingly, solution A experienced a lag period prior to coal dissolution, whereas dissolving lignite with solution B (CFF) shortened the coal dissolution time to 4 hours. Therefore, the CFF from *P. ortum* MJ51 was used to extract HAs.

Coal solubilization depends on the concentration of extracellular secondary metabolites of fungi, which are associated with the fungal growth period.[38] Thus, we studied the growth curve of *P. ortum* MJ51 and further explored the relationship between the pH of the CFF and the A_{450} value of the bio-solubilized products. The growth of *P. ortum* MJ51 changed over time and was divided into four stages: the lag phase (0–12 hours), exponential phase (12–60 hours), stationary phase (60–96 hours) and death phase (96–168 hours) (Fig. 1a). As fermentation proceeded, the pH of the CFF increased from 6.05 to 8.17 during the exponential phase, then further increased slowly during the stationary and death phases (Fig. 1c). The trend in A_{450} was similar to that of the CFF pH, which indicates

that the alkaline substances secreted by *P. ortum* MJ51 promote the release of HAs in coal. This result was supported by regression analysis (Fig. 1d), which showed a significant positive correlation between pH and A_{450} ($R^2 = 0.9098$, $p < 0.001$). Our results were consistent with those of previous studies.[15,39,40] Some microorganisms have been shown to secrete alkaline materials that increased the medium pH to more than 8 after 6 days;[15,22,41] however, the pH of the CFF from *P. ortum* MJ51 surpassed 8.0 after only 60 hours. This indicates that *P. ortum* MJ51 is more efficient than the previously used microorganisms for increasing the pH of the CFF, which is helpful for shortening the coal solubilization process.

3.1.2. Temperature effect. Solubilization of lignite by the CFF was investigated at various temperatures. The A_{450} value showed a continuous increasing trend in all treatments over 0–8 hours, but no notable increase was observed after 8 hours (Fig. 2a). With the increase of temperature (30–75 °C), the A_{450} value gradually increased, with a peak of 2.18 at 75 °C. A similar result was reported in a mechanically agitated tank reactor.[5] With the increase of temperature, a weak physical bond in the coal molecular structure was opened, the nonpolarity of the aqueous solution was stimulated, and the interaction between coal and water molecules was enhanced, which finally accelerated the dissolution of coal.[42] Based on the results of this study, a simple temperature increase did not cause a significant increase in the HA content in the blank medium solution; thus,
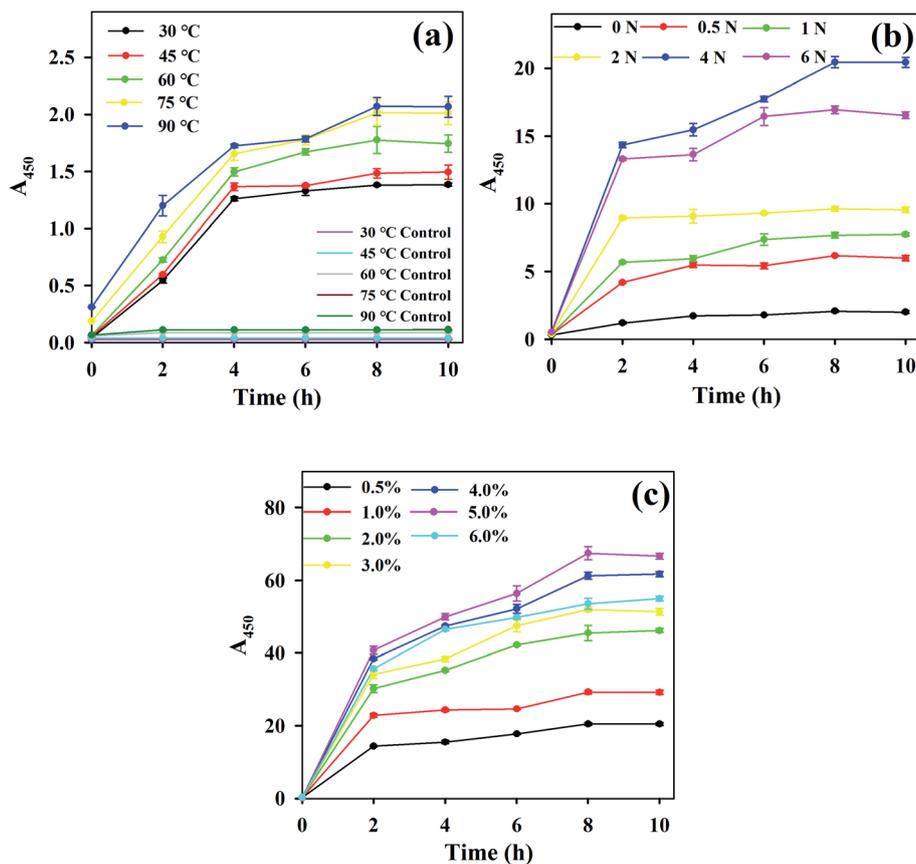
Fig. 2 Effect of different factors on coal solubilization. (a) Temperature, (b) HNO₃ concentration, and (c) coal loading ratio. Note: error bars indicate standard deviation.

it was speculated that CFF is the key to coal dissolution. We speculate that the reason for this may be that the elevated temperature greatly accelerates the reaction between alkaline and acidic groups, such as the hydroxyl and carboxyl groups in the coal, rather than only the reaction between the coal and water molecules. While an excessive temperature (90 °C) may inactivate the enzymes in the CFF, causing loss of coal-degrading function; on the other hand, high temperature may degrade the amino acid structure in the HA molecular chain,[5] thus the increased HAs may be offset by their degradation. The above reasons may explain why the HA concentration did not change significantly ($p > 0.05$) in this study when the temperature was raised to 90 °C.

Generally, alkaline substances, surfactants and extracellular enzymes in CFF participate during lignite solubilization. Previous research demonstrated that the degradation capacity was dramatically decreased when the CFF of *P. decumbens* P6 was heated.[22] In this work, the CFF still had strong activity when heated to 90 °C, indicating that the solubilization mechanism of *P. ortum* MJ51 is different from that of *P. decumbens* P6, and that the main active substances of the CFFs were resistant to high temperature. Due to the fact that few enzymes can resist such high temperatures and gradually increase in pH of CFF, we speculated that the main CFF substances contributing to coal solubilization were alkaline substances or surfactants; similar results have been found in the CFF from bacteria.[15,43] Currently,

the reported bacterial metabolites with coal-dissolving function include glycerophosphocholine, proveratrol A, proveratrol B and surfactin, *etc.*[44] To evaluate the composition of alkaline substances in the CFF of this study, whole genome-sequencing of *P. ortum* MJ51 was conducted. A large quantity of genes involved in aromatic compound degradation and alkaloid (isoquinoline, tropane, piperidine and pyridine alkaloid, pyridine and indole diterpene alkaloid *etc.*) biosynthesis were annotated (Fig. S1†). Living cells of *P. ortum* MJ51 depolymerize coal molecules by expressing genes involved in aromatic substance degradation, while CFF degrades coal mainly through alkaloids. Therefore, the coal solubilization mechanism by the CFF from *P. ortum* MJ51 was clarified.

3.1.3. HNO₃-pretreated coal effect. The effect of HNO₃-pretreated coal on the release of HAs was investigated at 75 °C (Fig. 2b). The A_{450} value continuously increased following an increase in the HNO₃ concentration (0–4 N) and time (0–10 hours), with a maximum value of 20.45 observed for 4 N HNO₃ at 8 hours, which was 10 times higher than the results obtained with raw coal. After the HNO₃ concentration exceeded 4 N, the A_{450} value declined. This is similar to the reported *Streptomyces fulvissimus* K59-mediated coal bio-solubilization, where the highest HA content was obtained with 5 N HNO₃-pretreated coal, relative to 2 N and 8 N HNO₃-pretreated coal.[18] A previous study of brown coal oxidation mechanisms by HNO₃ demonstrated that some inorganic substances inlaid in coal are acid-

Table 4 ANOVA of response surface quadratic model for humic acids production

Source	Sum of squares	df	Mean square	F-Value	p-Value
Model	4809.38	14	343.53	83.35	<0.0001
A – HNO$_3$ concentration	1698.84	1	1698.84	412.20	<0.0001
B – temperature	150.45	1	150.45	36.50	<0.0001
C – coal loading ratio	60.44	1	60.44	14.66	0.0018
D – time	99.65	1	99.65	24.18	0.0002
AB	20.16	1	20.16	4.89	0.0441
AC	2.94	1	2.94	0.71	0.4124
AD	3.15	1	3.15	0.76	0.3967
BC	1.72	1	1.72	0.42	0.5292
BD	2.24	1	2.24	0.54	0.4736
CD	4.84	1	4.84	1.17	0.2968
A^2	2622.28	1	2622.28	636.26	<0.0001
B^2	270.29	1	270.29	65.58	<0.0001
C^2	408.95	1	408.95	99.23	<0.0001
D^2	136.15	1	136.15	33.03	<0.0001
Residual	57.70	14	4.12		
Lack of fit	51.39	10	5.14	3.26	0.1332
Pure error	6.31	4	1.58		
Cor total	4867.08	28			
Coefficient of determination (R^2) = 0.9881					

soluble and that their removal reduces the ash content while concomitantly enhancing the pore volume and pore size of the coal. In addition, aromatic rings are opened and oxidized by nitric acid, which leads to an increase in carboxyl and a decrease in the aromaticity of HNO$_3$-oxidized coal.[45] An increased coal surface area and looser coal structure might facilitate its subsequent bio-liquefaction and promote the release of HAs from coal, while the oxidation of coal with 6 N HNO$_3$ led to a lower HA concentration in this study. Excessive oxidation of lignite decreases the C content and increases the carboxyl content and H/C ratio in residual coal.[18] A lower carbon content in lignite may lead to less organic substances in the coal dissolution products, while a higher carboxyl content and H/C ratio in the lignite could deplete more alkaline substance in the CFF and decrease the pH of the reaction liquid, thereby inhibiting the release of HAs from lignite.

3.1.4. Coal loading ratio effect. The effect of the coal loading ratio on coal solubilization was explored at 75 °C with 4 N HNO$_3$-pretreated coal. The A_{450} value of all treatments increased rapidly during 0–8 hours, and then remained basically constant at 10 hours (Fig. 2c). Properly increasing the coal loading ratio contributed to an increased HA concentration. A maximum A_{450} value of 67.49 was obtained at coal loading ratio of 5%. When the coal loading ratio increased to 6%, the HA concentration tended to decrease. Abundant carboxylic acid groups are introduced during nitric acid pretreatment.[40] The presence of excessive acidic groups would neutralize the alkalinity of the CFF, reduce the dissolution efficiency of coal, and finally decrease the HA concentration.

The same trend has been found during the coal dissolution process by living organisms. Under such conditions, previous studies have shown that the best coal loading ratio is 1%, which greatly limits the acquisition of fermentation products with
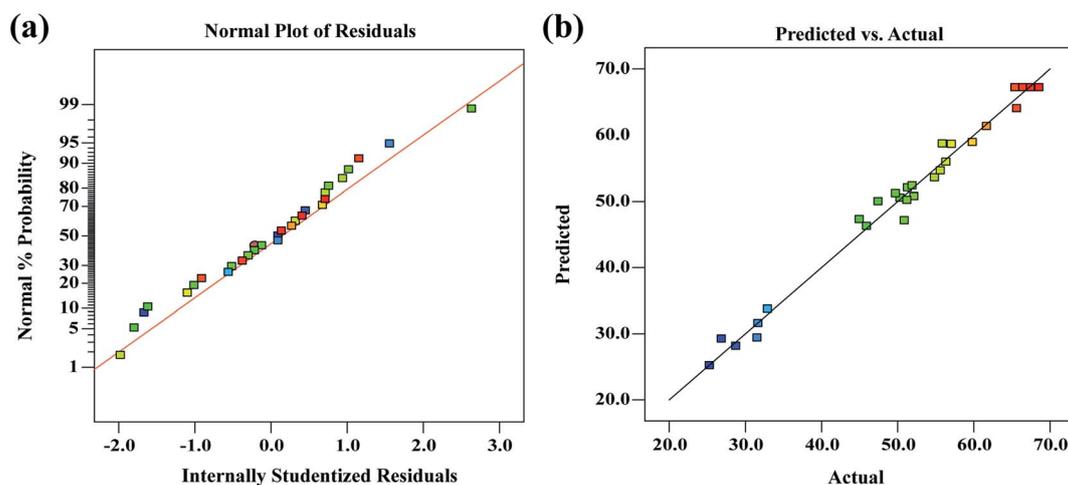

Fig. 3 Diagnostics of response surface quadratic model. (a) Normal plot of residuals, and (b) actual and predicted plot.

a high HA concentration.[38,46] The reason for this is that the presence of too much pulverized coal will cause cell damage and inhibit the activity of cells and enzymes related to coal degradation.[17] Conversely, CFF has a stronger tolerance to coal than living cells during the coal degradation process; thus, CFF can withstand greater coal addition, which provides greater potential for an improved HA concentration in fermentation products.

3.2. HA concentration optimization by RSM

In the present study, optimization of process parameters was carried out *via* Box–Behnken design to maximize the HA concentration. The following regression equations for coded values (eqn (4)) and actual experimental values (eqn (5)) were set up by collecting the data from actual experimental conditions (Table 3) according to the Box–Behnken model, which expresses the relationship between the dependent variable Y (the A_{450}
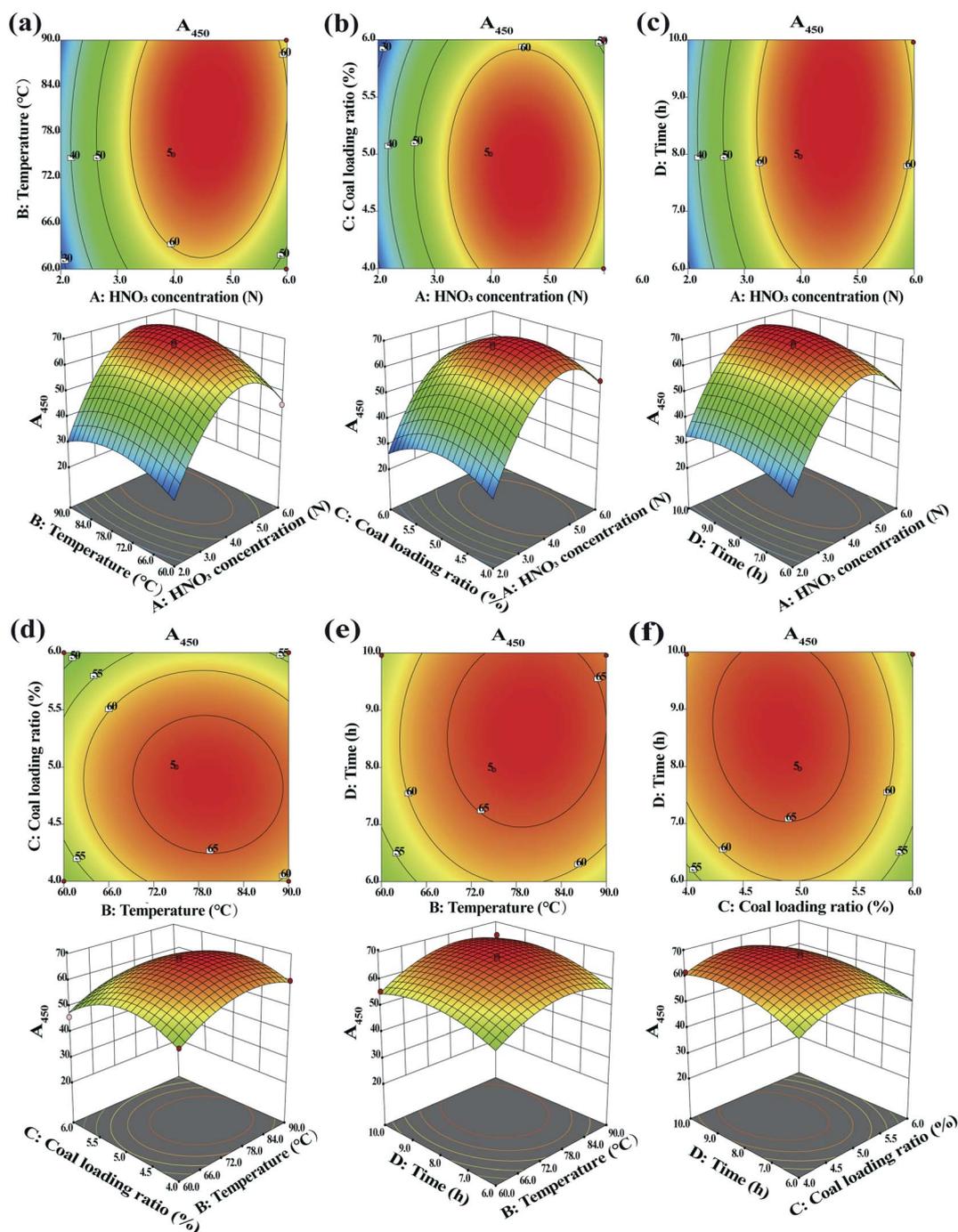

Fig. 4 Contour plots and 3-D surface plots of different variables interaction on HA concentration. (a) HNO_3 concentration and temperature; (b) HNO_3 concentration and coal loading ratio; (c) HNO_3 concentration and time; (d) temperature and coal loading ratio; (e) temperature and time; (f) coal loading ratio and time.

value) and the independent variables A (HNO$_3$ concentration), B (temperature), C (coal loading ratio) and D (time).

$$Y = 67.21 + 11.90A + 3.54B - 2.24C + 2.88D + 2.24AB - 0.86AC + 0.89AD - 0.66BC + 0.75BD + 1.10CD - 20.11A^2 - 6.46B^2 - 7.94C^2 - 4.58D^2 \tag{4}$$

$$Y = -490.66 + 40.92A + 4.26B + 86.55C + 19.76D + 0.07AB - 0.43AC + 0.22AD - 0.04BC + 0.02BD - 0.55CD - 5.03A^2 - 0.03B^2 - 7.94C^2 - 1.15D^2 \tag{5}$$

Analysis of variance (ANOVA) has been suggested as a way to examine the significance and accuracy of the quadratic model by RSM. The ANOVA results for the current optimization case are presented in Table 4. The F-value of the model was 83.35 and the p-value was less than 0.0001, which indicates that the regression model was extremely significant since the term is considered significant when the "P-value" is less than 0.05.[27] Furthermore, A, B, C, D, AB, A^2, B^2, C^2 and D^2 were also seen as significant model terms. The value of the "lack of fit" denotes the fitting degree of the current model and actual results.[26] In this study, the lack of fit value was 0.1332, which was larger than 0.05, so the current model can be considered to have a good confidence level. The coefficient of determination (R^2) of a good statistical model should be greater than 0.75, and explains a best fitting degree of regression equation to data.[27] In this case, the R^2 value of 0.9881 indicates that the model showed a good fit in the test range (Table 4). In addition, the normal probability and residual plots for the A_{450} value (Fig. 3a) further analyzed the adequacy of the fitted model. Meanwhile, predicted and measured values were virtually identical (Fig. 3b), which shows that the experiment design was appropriate.

Fig. 4 shows the contour plot and 3-D surface for the HA concentration (quantified with the A_{450} value) as a function of the HNO$_3$ concentration, temperature, coal loading ratio and time, as imitated by eqn (5). Color changes from blue to red indicate increasing HA concentrations. The shape of the contour plot can determine the intensity of the interaction effects, with an ellipse indicating significant interaction effects and a circle indicating the opposite.[47] With the increasing HNO$_3$ concentration and temperature, the A_{450} value continuously increased until peaking, and then decreased (Fig. 4a). The maximum A_{450} value was calculated at an HNO$_3$ concentration of 4.7 N and temperature of 77.3 °C. Moreover, a strong interaction was found between the HNO$_3$ concentration and temperature, as the two-dimensional contour plot was elliptical

with a large eccentricity (Fig. 4a). This observation was also validated *via* ANOVA (p-value of 0.0441 for AB) (Table 4). The A_{450} value followed a parabolic shape with an increase in the HNO$_3$ concentration and coal loading ratio (Fig. 4b). The maximum A_{450} value was calculated at an HNO$_3$ concentration of 4.7 N and a coal loading ratio of 4.9%. However, no significant interaction between the HNO$_3$ concentration and coal loading ratio was observed. This result was further confirmed *via* ANOVA (p-value of 0.4124 for AC) (Table 4). The contour plots and response surface plots for the effects of time and HNO$_3$ concentration, coal loading ratio and temperature, time and temperature, and time and coal loading ratio on the HA concentration (Fig. 4c–f, respectively) shared the same trend as that in Fig. 4b.

Through RSM, the optimum response value (A_{450} = 70.23) was achieved at an HNO$_3$ concentration of 4.7 N, coal loading ratio of 4.9%, time of 8.6 hours and temperature of 77.3 °C. In order to compare this with the predicted value, the experiment was repeated under the determined optimum conditions. A very similar A_{450} value of 70.28 was observed, thereby demonstrating that these optimization conditions had good repeatability.

3.3. Concentration and extraction yield of HAs

After optimization of HA extraction conditions, the concentration of HAs increased considerably from 0.71 g L^{-1} to 31.3 g L^{-1}, and the HA extraction yield increased from 14.1% to 63.9% (Table 5). Under the same extraction conditions, the yield of HAs extracted from raw lignite and HNO$_3$-pretreated lignite with NaOH solution was 58.7% and 66.4%, respectively. In our study, the extraction yield of HAs from lignite by the newly optimized method was comparable to that by the chemical method. While in previous study the yield of HAs extracted by the biological method (36.4%) from HNO$_3$-treated coal was lower than that by the chemical method (54.2%).[9] This indicates that the CFFs of *P. ortum* MJ51 could directly replace sodium hydroxide to extract HAs.

3.4. Quality evaluation of HAs

Multiple chemical and spectral analyses were used for quality evaluation of HAs extracted from lignite using CFF (HA-CFF), with HAs extracted using NaOH solution as the control (HA-control). The elemental composition of HA-CFF was obviously different from that of the HA-control, with lower carbon (C) and sulfur (S) contents, and higher nitrogen (N), hydrogen (H) and oxygen (O) contents (Fig. 5a). This result is consistent with

Table 5 Concentration and extraction yield of humic acids under different conditions[a]

Extraction method	HNO$_3$ concentration (N)	Temperature (°C)	Coal loading ratio (%)	Time (h)	C_{HAs} (g L^{-1})	HA yield (%)
Fermentation broth	0	30	0.5	240	0.7 ± 0.1	14.1 ± 0.9
CFF	4.7	77.3	4.9	8.6	31.3 ± 1.9	63.9 ± 2.8
NaOH (0.1 M)	0	77.3	4.9	8.6	28.8 ± 1.3	58.7 ± 2.4
NaOH (0.1 M)	4.7	77.3	4.9	8.6	32.5 ± 2.1	66.4 ± 3.1

[a] Note: results are presented as the mean ± standard deviation.

previous reports.[7,48] The increased O content may be directly related to the addition of oxygen-containing functional groups in the macromolecule. The new N in the HAs produced microbiologically was in the form of free or ionized NH_2-groups of amino acids, and its amount was related to the N content initially present in the medium.[49]

The H/C ratio represents the degree of unsaturation in the HAs, with a high H/C ratio often representing small molecular and low aromaticity compounds. The O/C ratio reflects the proportion of oxygen-containing groups in organic matter. Previous research has revealed that fungal-transformed HAs have higher O/C and H/C ratios than raw coal-derived HAs,[48,50] which is consistent with our results (Fig. 5a). The N/C ratio reflects the N content in the organic material, the HA-CFF showed a higher N/C atomic ratio of 0.11 than the HA-control, while previous studies reported that the N/C value of lignite-derived HAs was usually less than 0.05.[51,52] The E_4/E_6 ratio is known as the humification index. Generally, the higher the E_4/E_6 ratio, the lower molecular mass and content of condensed aromatic rings.[7] In the spectroscopic estimations, the E_4/E_6 ratio was also higher for HA-CFF when compared to the HA-control, suggesting that the CFF may attack the aromatic structure of coal and decrease the HA molecular mass. In addition, the HPSEC results confirmed that the molecular weight of the HAs was reduced by the CFF. The lowest molecular weight elution peak (25.85 kDa) of HA-CFF was lower than that of HA-control

(28.38 kDa), while the highest molecular weight elution peak in HA-control was divided into two elution peaks (66.78 and 63.74 kDa) in HA-CFF (Fig. 5b). Low molecular HAs can enter root cells and directly elicit intracellular signals;[53] thus, HA-CFF may be more active in stimulating plant metabolism than HA-control.

When an HA product is applied to agriculture as a water-soluble fertilizer synergist, anions in the HAs easily form insoluble humic acid salts with calcium and magnesium ions, which will limit its application as a water-soluble fertilizer in drip irrigation or as a foliar fertilizer on leaf surface.[54] Accordingly, the flocculation limit was used to evaluate the anti-flocculation ability of the HAs. The flocculation limit value was significantly higher in HA-CFF when compared to HA-control (Fig. 5a), suggesting higher hydrophilicity of HA-CFF; that is, the larger the hydrophilic components in humic samples, the higher the activity of HAs on plant physiology.[55] Moreover, HA-CFF exhibiting high hydrophilicity and anti-flocculation is very suitable for the preparation of liquid fertilizer, particularly when mixed with various trace elements and applied to drip irrigation and sprinkler irrigation systems.

Both the spectra of HA-CFF and HA-control had similar primary absorption bands (Fig. 5c). The common peaks were: 3500–3300 cm^{-1} (O–H stretching in alcohols and phenols), 1720 cm^{-1} (carboxylic and carbonyl groups), 1380–1480 cm^{-1} (deformation vibrations of methylene and methyl groups) and
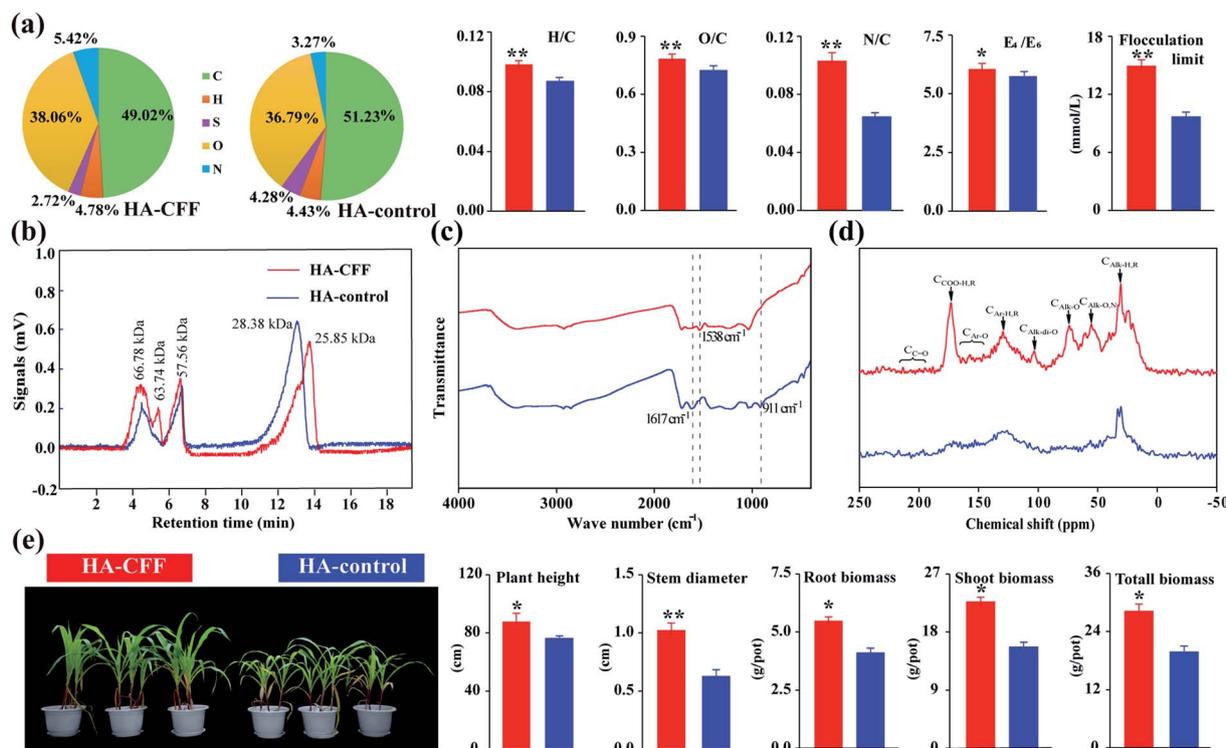

Fig. 5 Quality evaluation of humic acids. (a) Elemental composition, atomic ratio, E_4/E_6, and flocculation limit, (b) HPSEC elution profile, (c) FTIR spectra, (d) solid-state CP/MAS ^{13}C NMR spectroscopy and (e) plant physiological activity of humic acids. Note: HA-CFF, HA extracted by CFF; HA-control, HA extracted by NaOH. Error bars indicate standard deviation. Significant differences between treatments at $p < 0.05$ and $p < 0.01$ levels are labeled with * and **, respectively. In the (d), $C_{C=O}$ represents carbonyl C; $C_{COO-H,R}$ represents carboxyl C; C_{Ar-O} represents O-aromatic C; $C_{Ar-H,R}$ represents aromatic C; $C_{Alk-di-O}$ represents di-O-alkyl C (anomeric); C_{Alk-O} represents O-alkyl C; $C_{Alk-O,N}$ represents methoxyl and N-alkyl C; $C_{Alk-H,R}$ represents alkyl C.

Table 6 The distribution of carbon in HAs as determined by solid-state CP/MAS ^{13}C NMR spectroscopy[a]

ppm	190–220	160–190	140–160	110–140	90–110	60–90	45–60	0–45
	Carboxyl/carbonyl carbons		Aromatic carbons		Aliphatic carbons			
C%	$C_{C=O}$	$C_{COO-H,R}$	C_{Ar-O}	$C_{Ar-H,R}$	$C_{Alk-di-O}$	C_{Alk-O}	$C_{Alk-O,N}$	$C_{Alk-H,R}$
HA-control	2.0	8.8	10.0	26.9	4.0	8.0	7.2	32.9
HA-CFF	2.4	12.2	5.1	15.6	3.1	16.3	12.2	33.2

[a] Note: $C_{C=O}$ represents carbonyl C; $C_{COO-H,R}$ represents carboxyl C; C_{Ar-O} represents *O*-aromatic C; $C_{Ar-H,R}$ represents aromatic C; $C_{Alk-di-O}$ represents di-*O*-alkyl C (anomeric); C_{Alk-O} represents *O*-alkyl C; $C_{Alk-O,N}$ represents methoxyl and *N*-alkyl C; $C_{Alk-H,R}$ represents alkyl C.

1035 cm^{-1} (C–O stretch of polysaccharide-like components).[52,56] Compared with HA-control, the spectra of HA-CFF did not contain strong absorption bands in wavenumbers 1617 cm^{-1} and 911 cm^{-1}, which are assigned to stretching C=C groups in aromatic rings and aromatic C–H bending, respectively,[51] which suggests the collapse of aromatic rings. Conversely, HA-CFF had an absorption band at 1538 cm^{-1}, which was caused by C=N stretching and N–H deformation, implying that more N was introduced in HA-CFF.[57]

More detailed information on the structure of the HAs was obtained using solid-state ^{13}C CP/MAS NMR spectroscopy, which provides a non-destructive appraisal of the relative amounts of different structures in a sample. The spectra were divided into three regions: carboxyl/carbonyl carbons (160–220 ppm), aromatic carbons (110–160 ppm) and aliphatic carbons (0–110 ppm) (Table 6). The HA-CFF spectra were obviously different from those of HA-control (Fig. 5d), which contained more aliphatic carbon (C_{Alk-O} and $C_{Alk-O,N}$), carboxyl and ketone carbon ($C_{COO-H,R}$ and $C_{C=O}$), but less aromatic carbon (C_{Ar-O}, $C_{Ar-H,R}$ and $C_{Alk-di-O}$). These results were consistent with the results of the elemental analysis and FTIR. *O*-Alkyl groups play a positive role on root and coleoptile elongation.[29] The carboxyl (R–COOH) and hydroxyl (R–OH) groups of HAs play an important role in growth-related biological functions.[58] The physiological experiment also confirmed the stronger bioactivity of HA-CFF. The stem diameter, plant height, root biomass, shoot biomass and total plant biomass of maize were significantly higher for the HA-CFF treatment (Fig. 5e). These results reveal that HAs extracted using CFF have excellent chemical and physiological properties.

4. Conclusion

A new method to efficiently and cleanly convert lignite into HAs using fungal CFF was proposed. The HA production process was optimized by RSM, and the results showed that the maximum HA concentration of 31.3 g L^{-1} was achieved with 4.7 N HNO$_3$-pretreated lignite at a coal loading ratio of 4.9% and reaction temperature of 77.3 °C for 8.6 hours. The optimized method improved the HA extraction yield, shortened the reaction time and increased the coal loading ratio relative to the previous biological method. Quality evaluation showed that the HAs extracted from lignite using the CFF of *P. ortum* had a lower molecular weight, higher nitrogen and flocculation limit, and

stronger biological activity than the chemically-extracted HAs. In conclusion, the findings of this work could be a promising technique for biologically active HA production, as well as for clean utilization of lignite.

Author contributions

Shiying Li: experimental, data generation, writing – original draft. Jinfang Tan: conceptualization, review & editing. Yi Wang: investigation. Peipei Li: project administration. Desheng Hu: methodology. Qiuzhe Shi: draw the graphical abstract. Yanjun Yue: resources. Fang Li: methodology, writing – review & editing. Yanlai Han: conceptualization, review & editing, funding acquisition.

Conflicts of interest

The authors declare that they have no known competing financial interests or personal relationships that could have appeared to influence the work reported in this paper.

Acknowledgements

References

1 B. A. G. De Melo, F. L. Motta and M. H. A. Santana, *Mater. Sci. Eng., C*, 2016, **62**, 967–974.

2 T. A. van Tol De Castro, R. L. L. Berbara, O. C. H. Tavares, D. F. D. G. Mello, E. G. Pereira, C. D. C. B. Souza, L. M. Espinosa and A. C. García, *Plant Physiol. Biotechnol.*, 2021, **162**, 171–184.

3 Y. Li, F. Fang, J. Wei, X. Wu, R. Cui, G. Li, F. Zheng and D. Tan, *Sci. Rep.*, 2019, **9**, 12014.

4 M. Bahemmat, M. Farahbakhsh and M. Kianirad, *J. Hazard. Mater.*, 2016, **312**, 307–318.

5 E. Sarlaki, A. Sharif Paghaleh, M. H. Kianmehr and K. Asefpour Vakilian, *Renewable Energy*, 2021, **163**, 105–122.

6 N. Fatima, A. Jamal, Z. Huang, R. Liaquat, B. Ahmad, R. Haider, M. I. Ali, T. Shoukat, Z. A. ALOthman, M. Ouladsmane, T. Ali, S. Ali, N. Akhtar and M. Sillanpää, *Sustainability*, 2021, **13**, 8969.

7 M. J. Ghani, K. Akhtar, S. Khaliq, N. Akhtar and M. A. Ghauri, *Process Biochem.*, 2021, **107**, 1–12.

8 E. Sarlaki, A. Sharif Paghaleh, M. H. Kianmehr and K. Asefpour Vakilian, *J. Cleaner Prod.*, 2019, **235**, 712–723.

9 M. A. Sabar, M. I. Ali, N. Fatima, A. Y. Malik, A. Jamal, R. Liaquat, H. He, F. Liu, H. Guo, M. Urynowicz and Z. Huang, *Fuel*, 2020, **278**, 118301.

10 Y. Yang, J. Yang, B. Li, E. Wang and H. Yuan, *Fuel*, 2018, **214**, 416–422.

11 S. I. Zherebtsov, N. V. Malyshenko, L. V. Bryukhovetskaya and Z. R. Ismagilov, *Coke Chem.*, 2016, **58**, 400–403.

12 Z. Huang, C. Liers, R. Ullrich, M. Hofrichter and M. A. Urynowicz, *Fuel*, 2013, **112**, 295–301.

13 H. Machnikowska, K. Pawelec and A. Podgórska, *Fuel Process. Technol.*, 2002, **77**, 17–23.

14 M. S. Cohen and P. D. Gabriele, *Appl. Environ. Microbiol.*, 1982, **44**, 23–27.

15 F. Jiang, Z. Li, Z. Lv, T. Gao, J. Yang, Z. Qin and H. Yuan, *Fuel*, 2013, **103**, 639–645.

16 H. L. Yuan, J. S. Yang, F. Q. Wang and W. X, *Prikl. Biokhim. Mikrobiol.*, 2006, **42**, 59–62.

17 M. A. Sabar, M. I. Ali, N. Fatima, A. Y. Malik, A. Jamal, M. Farman, Z. Huang and M. Urynowicz, *Fuel*, 2019, **253**, 257–265.

18 J. Sobolczyk-Bednarek, A. Choińska-Pulit and W. Łaba, *Fuel*, 2021, **301**, 121082.

19 L. M. Sekhohola, E. E. Igbinigie and A. K. Cowan, *Biodegradation*, 2013, **24**, 305–318.

20 X. Feng, J. Sun and Y. Xie, *Fuel*, 2021, **291**, 120204.

21 J. K. Polman, K. S. Miller, D. L. Stoner and C. R. Breckenridge, *J. Chem. Technol. Biotechnol.*, 1994, **61**, 11–17.

22 H. Yuan, J. Yang and W. Chen, *Fuel*, 2006, **85**, 1378–1382.

23 G. Willmann and R. Fakoussa, *Fuel Process. Technol.*, 1997, **52**, 27–41.

24 A. Wali, I. Ben Salah, M. Zerrouki, A. Choukchou-Braham, Y. Kamoun and M. Ksibi, *Euro-Mediterranean Journal for Environmental Integration*, 2019, **4**, 1–9.

25 X. Song, J. Li, L. Chen, Z. Cai, C. Liao, H. Peng and H. Xiong, *J. Braz. Chem. Soc.*, 2012, **23**, 132–141.

26 C. Lu, Z. Zhang, X. Ge, Y. Wang, X. Zhou, X. You, H. Liu and Q. Zhang, *Int. J. Hydrogen Energy*, 2016, **41**, 13399–13407.

27 T. Lian, W. Zhang, Q. Cao, S. Wang, F. Yin, Y. Chen, T. Zhou and H. Dong, *Bioresour. Technol.*, 2021, **336**, 125307.

28 H. Monda, A. M. McKenna, R. Fountain and R. T. Lamar, *Front. Plant Sci.*, 2021, **12**, 958.

29 D. Savy, Y. Brostaux, V. Cozzolino, P. Delaplace, P. du Jardin and A. Piccolo, *Front. Plant Sci.*, 2020, **11**, 581.

30 L. Zhou, L. Yuan, B. Zhao, Y. Li and Z. Lin, *PLoS One*, 2019, **14**, e217469.

31 M. Arabi, A. Ostovan, A. R. Bagheri, X. Guo, J. Li, J. Ma and L. Chen, *Talanta*, 2020, **215**, 120933.

32 X. Song, J. Li, S. Xu, R. Ying, J. Ma, C. Liao, D. Liu, J. Yu and L. Chen, *Talanta*, 2012, **99**, 75–82.

33 P. Liu, Y. H. Liao, H. B. Zheng and Y. Tang, *Anal. Methods*, 2020, **12**, 2308–2316.

34 O. K. Achi, *Bioresour. Technol.*, 1994, **48**, 53–57.

35 J. K. Polman, D. L. Stoner and K. M. Delezene-Briggs, *J. Ind. Microbiol. Biotechnol.*, 1994, **13**, 292–299.

36 G. Zhou, J. Zhang, C. Zhang, Y. Feng, L. Chen, Z. Yu, X. Xin and B. Zhao, *Sci. Rep.*, 2016, **6**, 1–12.

37 M. S. Cohen, W. C. Bowers, H. Aronson and E. T. Gray, *Appl. Environ. Microbiol.*, 1987, **53**, 2840–2843.

38 R. Haider, M. A. Ghauri, E. J. Jones, W. H. Orem and J. R. SanFilipo, *Int. Biodeterior. Biodegrad.*, 2015, **100**, 149–154.

39 M. G. Baylon, Y. David, S. D. V. N. Pamidimarri, K. Baritugo, C. G. Chae, Y. J. Kim, T. W. Kim, M. Kim, J. G. Na and S. J. Park, *Korean J. Chem. Eng.*, 2017, **34**, 105–109.

40 D. R. Quigley, B. Ward, D. L. Crawford, H. J. Hatcher and P. R. Dugan, *Appl. Biochem. Biotechnol.*, 1989, **20–21**, 753–763.

41 N. Akimbekov, I. Digel, G. Abdieva, P. Ualieva and K. Tastambek, *Biofuels*, 2021, **12**, 247–258.

42 G. Cheng, Z. Niu, C. Zhang, X. Zhang and X. Li, *Appl. Sci.*, 2019, **9**, 1356.

43 I. Romanowska, B. Strzelecki and S. Bielecki, *Fuel Process. Technol.*, 2015, **131**, 430–436.

44 B. Wang, F. Ndayisenga, G. Zhang and Z. Yu, *GCB Bioenergy*, 2021, **13**, 967–978.

45 Y. Başaran, A. Denizli, B. Sakintuna, A. Taralp and Y. Yürüm, *Energy Fuels*, 2003, **17**, 1068–1074.

46 H. Kang, X. Liu, Y. Zhang, S. Zhao, Z. Yang, Z. Du and A. Zhou, *Energy Sources, Part A*, 2021, **43**, 1162–1180.

47 C. Lu, Y. Jing, H. Zhang, D. Lee, N. Tahir, Q. Zhang, W. Li, Y. Wang, X. Liang, J. Wang, P. Jin and X. Zhang, *Bioresour. Technol.*, 2020, **304**, 123007.

48 L. Dong, Q. Yuan and H. Yuan, *Fuel*, 2006, **85**, 2402–2407.

49 L. Dong and H. Yuan, *Geomicrobiol. J.*, 2009, **26**, 484–490.

50 R. Haider, M. A. Ghauri and K. Akhtar, *Geomicrobiol. J.*, 2015, **32**, 944–953.

51 Y. Zhang, Y. Li, L. Chang, C. Zi, G. Liang, D. Zhang and Y. Su, *RSC Adv.*, 2020, **10**, 22002–22009.

52 L. Doskočil, J. Burdíková-Szewieczková, V. Enev, L. Kalina and J. Wasserbauer, *Fuel*, 2018, **213**, 123–132.

53 S. Nardi, M. Schiavon and O. Francioso, *Molecules*, 2021, **26**, 2256.

54 T. Ahmad, R. Khan and T. Nawaz Khattak, *J. Plant Nutr.*, 2018, **41**, 2438–2445.

55 S. Nardi, A. Muscolo, S. Vaccaro, S. Baiano, R. Spaccini and A. Piccolo, *Soil Biol. Biochem.*, 2007, **39**, 3138–3146.

56 Z. Wang, T. Shen, Y. Yang, B. Gao, Y. Wan, Y. C. Li, Y. Yao, L. Liu, Y. Tang, J. Xie, F. Ding and J. Chen, *J. Cleaner Prod.*, 2020, **243**, 118585.

57 G. Ait Baddi, M. Hafidi, J. Cegarra, J. A. Alburquerque, J. Gonzálvez, V. Gilard and J. Revel, *Bioresour. Technol.*, 2004, **93**, 285–290.

58 M. Y. Byun, D. Kim, U. J. Youn, S. Lee and H. Lee, *Plant Physiol. Biochem.*, 2021, **159**, 37–42.